1962

Dynamic instability in barotropic flow

Haltiner, G.J.

Haltiner, G. J., and Song, R.T. "Dynamic instability in barotropic flow." Tellus 14.4 (1962): 383-393.
http://hdl.handle.net/10945/50456

Dynamic instability in barotropic flow

By G. J. HALTINER, *U. S. Naval Postgraduate School, Monterey, California*
and LT .R. T. SONG, *Korean Navy*

(Manuscript received July 9, 1962)

ABSTRACT

The dynamic stability of single-jet and double-jet zonal currents is investigated for several quasi-barotropic models by a finite difference method and by means of finite Fourier series.

The two methods give generally similar results, but some moderate differences occur when the mesh length is decreased or the number of Fourier components is increased. Also the stability characteristics of single-jet and double-jet profiles differ considerably.

1. Introduction

The primary purpose of this investigation is to determine the stability properties of quasi-barotropic currents by several approximation methods and compare the results. KUO (1949) gave the first detailed treatment of non-divergent barotropic flow and provided a necessary and sufficient condition for unstable waves in a jet-type current. ELIASSEN (1954) introduced a simpler approximation method to obtain the stability characteristics of some specific non-divergent currents. More recently WIIN-NIELSEN (1961) utilized Eliassen's method of finite Fourier series to determine the stability properties of the divergent one-parameter quasi-barotropic model for a jet-type current. He also considered the second-order changes and showed from the linear theory that a single-jet current would develop a double-jet structure as a result of meridional convergence of momentum by unstable eddies. The latter results were also verified by an extension of Lorenz's method of maximum simplification of the hydrodynamical equations, and in addition the transition from a double jet to a single jet was established.

In this paper the stability properties of the non-divergent, divergent, and the "stratified" (ARNASON 1961) quasi-barotropic models will be investigated for single- and double-jet zonal wind currents by a finite difference technique and by the finite Fourier series method.

2. The divergent one-parameter model

Following WIIN-NIELSEN (1959), the vorticity equation for the divergent one-parameter model may be written in the form

$$\frac{\partial}{\partial t}(\nabla^2\Psi) + \mathbf{V}\cdot\nabla(\nabla^2\Psi + f) = q^2\frac{\partial\Psi}{\partial t} \qquad (1)$$

Here $\mathbf{V} = \mathbf{k}\times\nabla\Psi$; Ψ is the stream function; and q^2, to be treated as a constant, is a parameter depending on the mean coriolis parameter, the static stability and the vertical variation of the wind near 500 mbs.

By application the method of small perturbations, equation (1) may be linearized and expressed in the form

$$\nabla^2\frac{\partial\Psi'}{\partial t} + U\frac{\partial}{\partial x}(\nabla^2\Psi') + \frac{\partial\Psi'}{\partial x}\left(\beta - \frac{d^2U}{dy^2}\right) = q^2\frac{\partial\Psi'}{\partial t}, \qquad (2)$$

where Ψ' is the perturbation stream function, and U is the zonal current, a function of y alone.

Next assuming the perturbation to be of harmonic form

$$\Psi'(x, y, t) = \phi(y)\, e^{i\mu(x-ct)} \qquad (3)$$

and substituting this into (2) yields a linear second-order differential equation,

$$(U-c)(\phi'' - \mu^2\phi) + (\beta - U'' + q^2c)\phi = 0; \qquad (4)$$

The prime here designates differentiation with respect to y, β is the Rossby parameter, $\mu = 2\pi/L$ with L the wave length, and c is the phase velocity, which may be complex,

$$c = c_r + ic_i.$$

The simplest boundary conditions that approximate actual conditions to some extent are that the perturbations vanish at two latitudes corresponding, say, to $y = 0$ and $y = D$, i.e.,

$$\phi(0) = \phi(D) = 0. \tag{5}$$

Of particular interest here is the characteristic value problem, namely, the determination of values of c for which solutions of the system (3), (5) exist. Even for rather simple functions $U(y)$, solutions in terms of elementary functions generally do not exist; although methods for finding infinite-series solutions are well known. The characteristic-value problem in the latter methods, however, is frequently very difficult. Hence it is desirable to attempt to approximate solutions by use of finite-difference or finite Fourier methods.

3. Method I. Method of finite differences

This method consists of dividing the basic interval D into n subdivisions of width d by $(n-1)$ equally spaced points within the fundamental interval, $O < y < D$. The derivatives of $\phi(y)$ are then approximated by the finite difference ratio

$$\phi_j'' = \frac{\phi_{j+1} - 2\phi_j + \phi_{j-1}}{d^2}, \tag{6}$$

where j represents any interior point of the interval. A similar representation may be used for U'' if so desired; however this will not be necessary for most of the examples considered here in which the zonal wind fields will be represented by analytic functions. In general it may be expected that the accuracy of the solutions obtained through the use of (5) will increase as the value of n increase; however the computational effort naturally increases with increasing n. For the cases considered here, n will be restricted to the values 6 and 8. Moreover, only zonal wind profiles which are symmetrical with respect to the center of the basic interval will be considered. Hence, since the β parameter is treated as a constant, the amplitude of the perturbation stream function may also be expected to be symmetrical with respect to the basic interval.

Case (A), $n = 6$.

First consider the case $n = 6$ and let the subscripts 0, 1 and 2 correspond to the points $\eta = D/2$, $2D/3$, and $5D/6$, respectively. Next, equation (4) is written for each of these points utilizing the finite difference approximation (6) for ϕ'', as appropriate. With the boundary condition $\phi(D) = 0$, the following system is obtained:

$$\begin{aligned}
&[(c-U_0)(2+\mu^2d^2) + d^2(\beta - U_0'') + d^2q^2c]\phi_0 \\
&\qquad + 2(U_0 - c)\phi_1 = 0 \\
&(U_1 - c)\phi_0 + [(c-U_1)(2+\mu^2d^2) + d^2(\beta - U_1'') \\
&\qquad + d^2q^2c]\phi_1 + (U_1 - c)\phi_2 = 0 \\
&(U_2 - c)\phi_1 + [(c-U_2)(2+\mu^2d^2) + d^2(\beta - U_2'') \\
&\qquad + d^2q^2c]\phi_2 = 0
\end{aligned} \tag{7}$$

For a known function U, the above equations constitute a linear homogeneous system in the "unknowns", ϕ_0, ϕ_1, and ϕ_2. The characteristic values of c may now be obtained by imposing the condition for a non-trivial solution for the ϕ's, namely, the determinant of the coefficients must vanish. The resulting frequency equation has the form

$$a_3c^3 + a_2c^2 + a_1c + a_0 = 0, \tag{8}$$

where

$$\begin{aligned}
a_3 &= h(h^2 - 3) \\
a_2 &= h[(P_1 + P_2)h + (U_1 + U_2)(1 - rh)] + (h^2 - 1) \\
&\quad (P_0 - U_0r) + 2h(U_0 + U_1) - 2(P_2 - U_2r) \\
a_1 &= h[U_1U_2(r^2 - 1) + P_1P_2 - r(P_1U_2 \\
&\quad + P_2U_1)] + [h(P_1 + P_2) + (U_1 + U_2) \\
&\quad (1 - rh)](P_0 - U_0r) - 2hU_0U_1 \\
&\quad + 2(U_0 + U_1)(P_2 - U_2r) \\
a_0 &= [U_1U_2(r^2 - 1) + P_1P_2 - r(P_1U_2 + P_2U_1)] \\
&\quad [P_0 - U_0r] - 2U_0U_1(P_2 - U_2r)
\end{aligned} \tag{9}$$

$$P_j = d^2(\beta - U_j''),\ h = r + d^2q^2, \text{ and } r = 2 + \mu^2d^2$$

Since (8) is a cubic equation, in general there exists 3 roots, which may include a pair of conjugate complex values. Equation (8) has been solved numerically on a Control Data Corporation 1604 computer, using the MULLER method (1956), for several zonal wind profiles

and for a variety of values of the parameters, D, L, q, and β.

Example I. Single-jet basic current

The first example considered is the single-jet zonal wind profile used by Wiin-Nielsen (1961), namely,

$$U = B\left(1 - \cos\frac{2\pi}{D}y\right) \tag{10}$$

which is shown as curve (2) in figure 1. The value of B is 30 m/sec, implying a rather intense jet with a maximum wind speed of 60 m/sec. The results are shown in figures 2 and 3 which give only the imaginary part of c as a function of wave length L for $D = 2000$ km, and $D = 4000$ and $D = 6000$ km, respectively. Each figure contains a number of curves corresponding to different values of β and divergence, as represented by q^2. From figures 2 and 3 the following conclusions are evident:

(*a*) the β parameter has a stabilizing influence in the sense that the magnitude of c_i is less for $\beta = \beta_{45}$ than for $\beta = 0$, and also the band of unstable wave lengths is narrower.

(*b*) divergence, as represented by the parameter q^2, has a stabilizing influence with c_i decreasing with increasing q^2.

(*c*) the wave length of maximum instability shifts toward shorter wave lengths with increasing q^2 and β;

(*d*) the instability decreases with increasing width of the channel D, except possibly for the case $\beta = q^2 = 0$, but the wave length of maximum instability increases with increasing D;

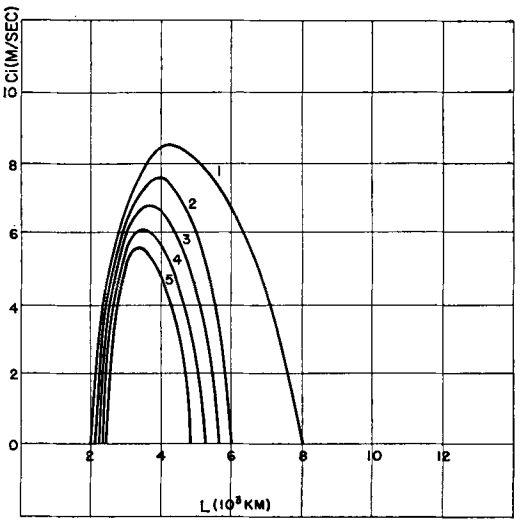

FIG. 2. c_i as a function of L for $U = B(1 - \cos(2\pi/D)y)$ with $n = 6$, $B = 30$ m/sec, $D = 2000$ km and Curve 1: $\beta = 0$, $q^2 = 0$; curve 2: $\beta = \beta_{45}$, $q^2 = 0$; curve 3: $\beta = \beta_{45}$, $q^2 = 0.5 \times 10^{-12}$ m^{-2}; curve 4: $\beta = \beta_{45}$, $q^2 = 1.0 \times 10^{-12}$ m^{-2}; curve 5: $\beta = \beta_{45}$, $q^2 = 1.5 \times 10^{-12}$ m^{-2}.

(*e*) the unstable waves are generally found for intermediate wave lengths with very long and short waves stable, similar to baroclinic instability and in general agreement with the average wave length of observed synoptic waves.

Example II. $U_0 = 2B$, $U_1 = B$, $U_2 = B/2$

Figure 4 shows the results for a somewhat more pointed single-jet profile where the velocity at $y = 2/3$ D is 1/3 less than for the

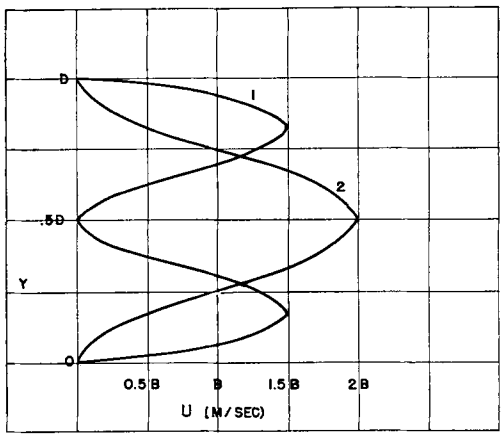

FIG. 1. Zonal wind profiles: Curve 2, $U = B(1 - \cos(2\pi/D)y)$; Curve 1, $U = B\,(\sin(\pi/D)y + \sin(3\pi/D)y)$.

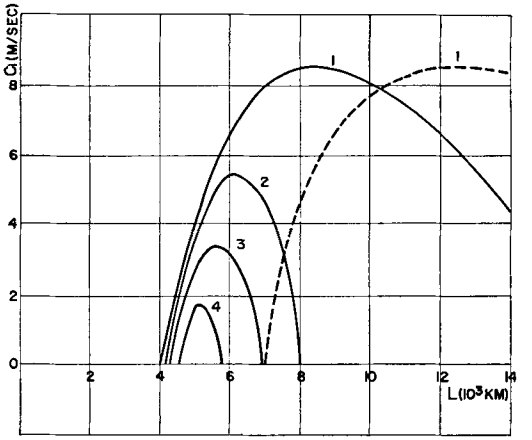

FIG. 3. Similar to figure 2 except that $D = 4000$ km; dashed curve corresponds to $D = 6000$ km.

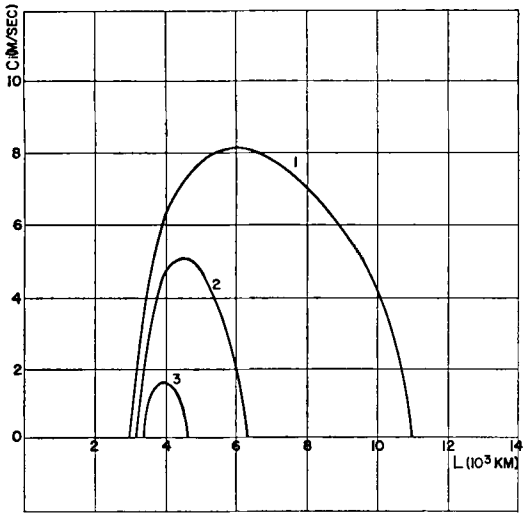

FIG. 4. Similar to figure 2 except that $U_0 = 2B$, $U_1 = B$, $U_2 = B/2$ and $D = 4000$.

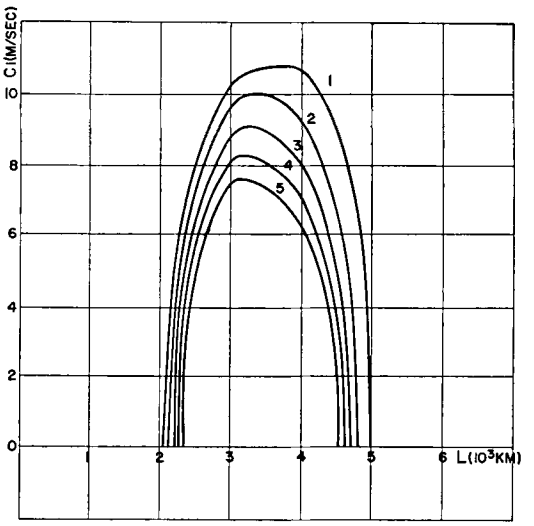

FIG. 5. Similar to figure 3 except that $U = B(\cos(4\pi/D)y - \cos(2\pi/D)y)$, (horizontal scale expanded).

previous case. As might have been expected from the variation with D in the previous example, the instability is somewhat less here than for the corresponding values in the first case; however, the general characteristics are similar.

Example III. $U = B\left(\cos\frac{4\pi}{D} - \cos\frac{2\pi}{D}y\right)$

This zonal profile also has a rather sharp single-jet of westerlies but possess a band of easterly winds on either side. The stability characteristics for $D = 4000$ km, as displayed in figure 5, are similar to the cases already shown; but, when compared to figure 3, the magnitude of c_i is seen to be larger for all curves. However, curves (1) and (2) show a narrower band of instability than previously. The curves for 2000 km and 6000 km are not shown; but as D increases there is a decrease in the width of the band of unstable wavelengths, a shift of this band toward longer wavelengths and a sharper decrease of the magnitude of c_i with increasing β and q^2.

Example IV. Double-jet basic current

A quite common occurrence observed on synoptic maps is the split of the isotach maximum so that maxima of wind speed are found at two different latitudes. Hence it is of interest to examine the stability properties of a double-jet zonal current. The profile chosen for this example is represented by

$$U = B\left(\sin\frac{\pi}{D}y + \sin\frac{3\pi}{D}y\right), \qquad (11)$$

which is shown as curve (1) in figure 1. Utilizing the expression in equation (8) and carrying out a similar series of computations with $B = 40$ m/sec. yielded the results shown in figure 6 and 7, corresponding to $D = 2000$ and 4000 km, respectively.

The general shape of the curves in figure 6 and 7 is similar to the results of the previous curves, however contrary to Example I, β and q^2 do not exhibit a stabilizing influence for all wavelengths. Instead, for wavelengths longer than that corresponding to the maximum instability, the value of c_i increases for the larger values of β and q^2; thus the latter have a destabilizing influence there. Moreover, the band of unstable wavelengths broadens with increasing β and q^2 in addition to showing the previously implied shift of maximum instability toward slightly longer wavelengths.

Figure 7 shows a somewhat more complicated set of curves than heretofore; however, qualitatively, the deviations from the single-jet case are similar to those described for figure 6. The primary differences from the latter are firstly, the appearance of two maxima of c_i with respect to wavelength; and secondly, the pro-

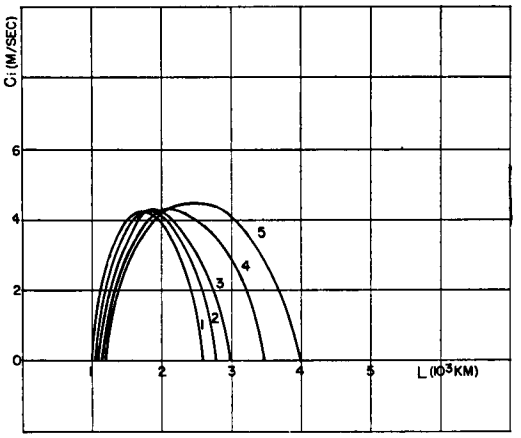

FIG. 6. Similar to figure 2 except that $U = B(\sin(\pi/D)y + \sin(3\pi/D)y)$, $B = 40$ m/sec, horizontal scale expanded.

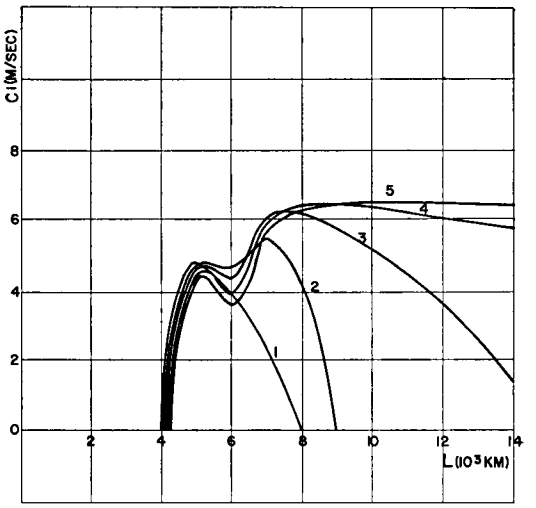

FIG. 7. Similar to figure 6 with $D = 4000$ km.

nounced broadening of the band of unstable wavelengths for the larger value of D. Thus the stability characteristics of the double-jet profile appear quite different in many respects from those of the single-jet case.

A word of caution should be injected here, however, for it must be remembered that a finite difference approximation for derivatives is being used to reduce the differential equation (4) to the linear algebraic system (7), and the subdivision of the channel into 6 mesh lengths is probably a cruder representation for the double-jet current than for the simpler single-jet case, giving rise to larger truncation errors. Case B), $n = 8$.

As a check on the previous results the mesh size was decreased by dividing the basic interval into 8 subdivisions. In this event equation (4) is applied at 4 interior points leading to a linear system of 4 equations in ϕ_j, $j = 0, 1, 2, 3$, analogous to (7). The condition that the determinant vanish for a non-trivial solution leads to a quartic equation for c.

Example I. Single-jet basic current, equation (10).

The values of c_i as a function of wavelength for $D = 4000$ km and the same series of values of β and q^2 are shown in figure 8. Only one pair of conjugate complex roots resulted in each case and these were quite similar to the case, $n = 6$. A comparison of figures 8 and 3 reveals the following differences:

(*a*) with $n = 8$, there is a shift of curve 1 (for $\beta = q^2 = 0$) toward somewhat longer wavelengths; and, comparing curves (2) and (3), β appears to have a destabilizing influence on the shorter unstable waves;

(*b*) the band of unstable waves is slightly broader and the magnitude of c_i is somewhat larger for $n = 8$ than for $n = 6$;

(*c*) the curve for $D = 2000$ and $D = 6000$ km, which are not given, show the previous decrease in instability with increasing D and the shift of the instability toward longer wavelengths.

For somewhat more detail regarding the phase velocities, consider the specific values for $D = 4000$ km, $\beta = \beta_{45}$, $q^2 = .5 \times 10^{-10}$ m^{-2} and $L = 6000$ km:

$$n = 6: \quad c_{1,2} = 15.51 \pm 3.2i,$$
$$c_3 = 41.87, \text{ (m/sec)},$$

$$n = 8: \quad c_{1,2} = 12.93 \pm 4.06i,$$
$$c_3 = 29.67, \; c_4 = 49.65, \text{ (m/sec)}$$

Thus the single real root for $n = 6$ lies between the pair of real roots for $n = 8$; also the complex roots differ somewhat.

Example IV. Double-jet basic current, equation (11), $n = 8$.

As suggested earlier, greater differences between the cases $n = 8$ and $n = 6$ might well be expected in the double-jet profile than the single-jet because of its greater complexity. Figure 9, which shows the results for $D = 4000$

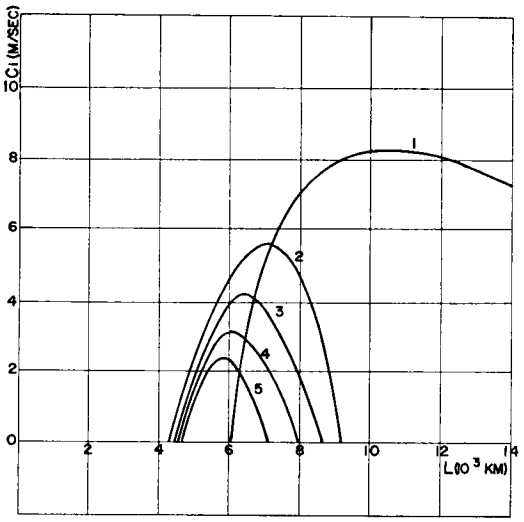

FIG. 8. Similar to figure 3 with $n = 8$.

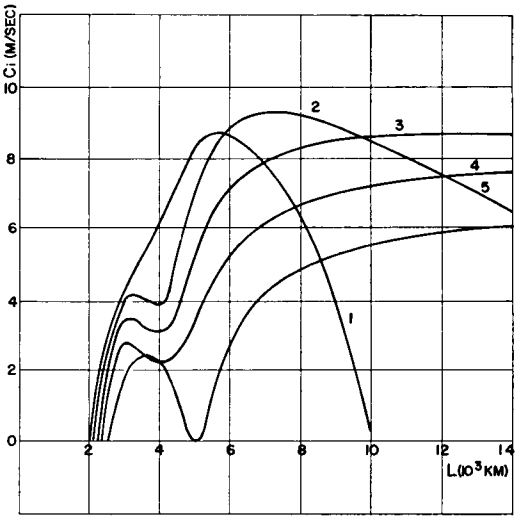

FIG. 9. Similar to figure 6 with $n = 8$.

($n = 8$), is fairly similar to figure 7 ($D = 4000$, $n = 6$), except as follows:

a) the magnitude of c_i is generally somewhat larger in curves 1, 2 and 3 and the band of unstable wavelengths is somewhat broader.

b) curves 3, 4 and 5 indicate that an increasing q^2 has a stabilizing influence; however, a comparison of the slopes suggests that this effect will reverse at sufficiently longer wavelengths.

4. Method II. Finite Fourier series method

When trigometric functions are used to represent the zonal wind, it is logical to consider a Fourier series representation for ϕ (y). Because of the assumed symmetry of this function, the special character of the differential equation (4) and the type of zonal wind profile used here, either an even or an odd set of functions may be used. Consider a solution of the form

$$\phi(y) = \sum_{j=1}^{N} \phi_j \sin j\lambda y, \quad j = 1, 3, 5, \ldots N, \qquad (12)$$

where $\lambda = \pi/D$. The expression (12) obviously satisfies the boundary conditions (5). The reliability of the results may be expected to increase with increasing N.

WIIN-NIELSEN (1961) has present the stability characteristics for the zonal wind profile (10) for the case $N = 3$. Larger values of N (including even values) have been considered by ELIASSEN (1954), but with divergence excluded, and mainly for $\beta = 0$. Eliassen found only one pair of conjugate complex values of c corresponding to odd values of j.

Here odd values of j will be of primary concern with $N = 5$ and $N = 7$.

Example I. Single-jet basic current, equation 10, $N = 5$.

Inserting (12) into equation (4), obtaining a series in terms of the elementary functions sin λy, sin $3\lambda y$, etc., and finally equating the coefficients of these terms to zero, leads to a linear homogeneous system of equations for the corresponding ϕ_1, ϕ_3, etc., namely,

$$\begin{aligned}
&[(\lambda^2 + \mu^2 + q^2)c + \beta - (1/2)B(3\mu^2 - \lambda^2)]\phi_1 \\
&\quad + [(1/2)B(5\lambda^2 + \mu^2)]\phi_3 = 0 \\
&[(1/2)B(\mu^2 - 3\lambda^2)]\phi_1 + [(9\lambda^2 + \mu + q^2)c + \beta - \\
&\quad - B(9\lambda^2 + \mu^2)\phi_3 + (1/2)B(21\lambda^2 + \mu^2)]\phi_5 = 0 \qquad (13) \\
&[(1/2)B(5\lambda^2 + \mu^2)]\phi_3 + [(25\lambda^2 + \mu^2 + q^2)c \\
&\quad + \beta - B(25\lambda^2 + \mu^2)]\phi_5 = 0
\end{aligned}$$

Setting the determinant equal to zero as before gives a cubic frequency equation for the phase velocity c.

$$\begin{aligned}
&c^3(RWE) + c^2[E(RV + SW) + RWG] + c[E \\
&(SV - TH) + G(RV + SW) - PHW] + G(SV \\
&\quad - TH) - PHV = 0,
\end{aligned}$$

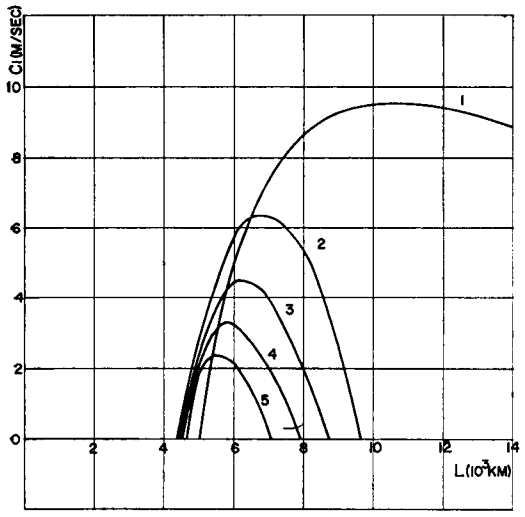

FIG. 10. Similar to figure 3 with $N=5$ (Fourier method).

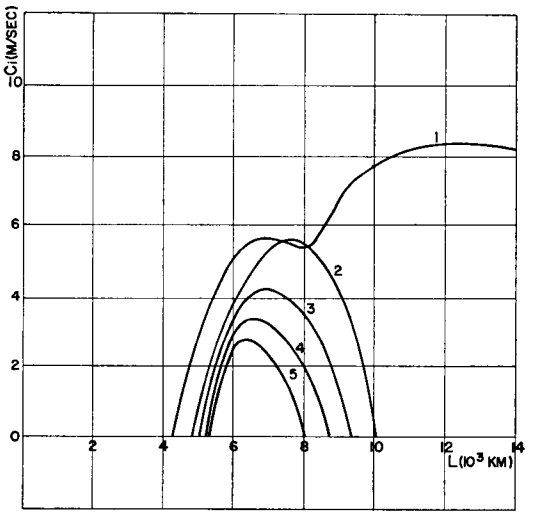

FIG. 11. Similar to figure 10 with $N=7$ (Fourier method).

where

$$E=\lambda^2+\mu^2+q^2, \qquad G=\beta-1/2B(3\mu^2-\lambda^2),$$
$$H=1/2B(5\lambda^2+\mu^2), \qquad P=1/2B(\mu^2-3\lambda^2),$$
$$R=8\lambda^2+E \qquad S=\beta-B(9\lambda^2+\mu^2)$$
$$T=1/2B(21\lambda^2+\mu^2), \qquad W=24\lambda^2+E$$
$$V=\beta-B(25\lambda^2+\mu^2)$$

When $N=7$, a similar procedure leads to a system of four linear homogeneous equations in the amplitudes $\phi_1,\phi_3,\phi_5,\phi_7$ and a quartic equation in c.

Figure 10 gives c_i as a function of wavelength for the single-jet profile (equation 10) for $N=5$, $D=4000$ and various values of β and q^2; and figure 11 gives similar results for $N=7$. At most one pair of conjugate imaginary roots for c appeared in the latter case.

There is obviously a close similarity in the essential features between the cases $N=5$, $N=7$. Moreover, these results correspond closely to those of the finite difference method, particularly between the latter case for $n=8$ (figure 8) and the Fourier method for $N=5$ (figure 10), but also between the finite difference case

TABLE 1. *Phase velocity c (m/sec) for single-jet basic current as obtained by Fourier method for $N=5$ and $N=7$ with $D=4000$ km, $\beta=\beta_{45}$, and $q^2=.5\times10^{-12}$ m^{-2}; wave-length L is given in units of 1000 km.*

	N = 5			N = 7			
L	C_1	C_2	C_3	C_1	C_2	C_3	C_4
1	11.80	35.61	54.47	7.72	24.49	43.56	55.67
2	12.71	33.50	48.74	8.76	23.96	40.70	50.74
3	13.58	30.24	42.90	9.61	23.26	35.84	47.13
4	14.63	24.67	39.23	10.38	21.75	29.91	45.54
5	$16.77\pm2.75i$		37.52	11.68	17.25	26.32	44.84
6	$13.97\pm4.48i$		36.68	$11.99\pm3.50i$		25.18	44.46
7	$11.51\pm4.06i$		36.20	$9.62\pm4.22i$		24.75	44.24
8	$9.44\pm1.81i$		35.90	$7.58\pm3.54i$		24.53	44.10
9	3.90	11.54	35.70	$5.87\pm1.11i$		24.40	44.00
10	.47	12.14	35.57	.89	8.04	24.31	44.93
11	−2.16	12.43	35.47	−1.94	8.54	24.25	43.88
12	−4.27	12.61	35.39	−4.13	8.80	24.21	43.84

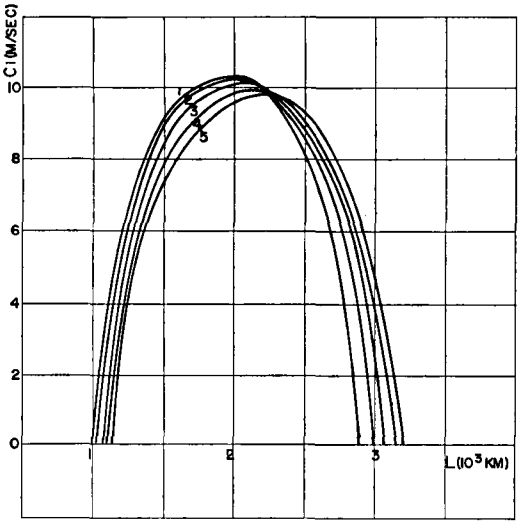

FIG. 12. Similar to figure 2 with $U = B(1 - \cos(4\pi/D)y)$, $D = 2000$ km and $N = 5$. (Fourier method), horizontal scale expanded.

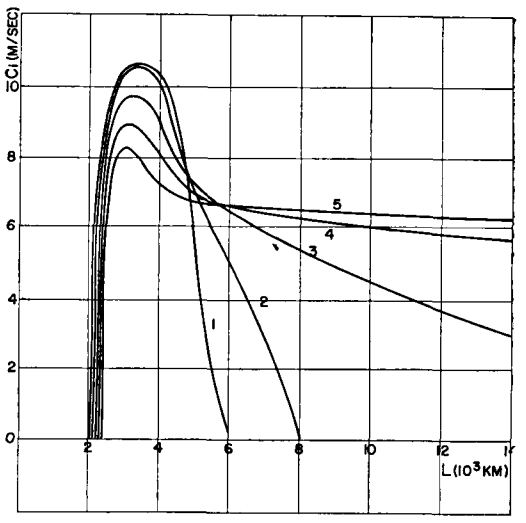

FIG. 13. Similar to figure 12 with $D = 4000$ km.

$n = 6$ (figure 3) and Wiin-Nielsen's results for $N = 3$. The following differences may be noted, except possibly for $\beta = q^2 = 0$,

(*a*) the maximum c_i decreases slightly, but the band of unstable waves becomes a little broader as N increases;

(*b*) the wavelength for the maximum c_i shifts slightly toward somewhat longer wavelengths as N increases.

As a further comparison between the results of the Fourier method for $N = 5$ and $N = 7$, the roots of the frequency equations are provided in Table I for the case, $D = 4000$ km, $\beta = B_{45}$, and $q^2 = .5 \times 10^{-12}$ m^{-2} for wavelengths of 1000 to 12,000 km. Though quite similar, the differences here are somewhat greater than noted by Eliassen.

Example V. A slightly different double-jet basic current is examined next as represented by the equation

$$U = B\left(1 - \cos\frac{4\pi}{D}y\right), \qquad (15)$$

where again B is 30 m/sec. This current is zero at the center of the channel, as well as at both lateral boundaries, and has value $2B$ at $y = D/4$ and $3D/4$. It is shown as U (0) in figure (16). Figure 12 (horizontal scale expanded) gives c_i as a function of wavelength for $D = 2000$ km. Here the band of unstable wavelengths is rather narrow and confined to rather short waves; also the variation with different values of β and q is negligible. Figure 13 shows the results for $D = 4000$, which indicates broader instability with shift toward longer wavelengths and also a greater variation of stability with β and q. A comparison of figures 9 and 13 shows that what appears to rather minor changes in the shape of the basic wind profile, together with the difference due to method, can give moderate differences in the instability characteristics.

5. The stratified model

ARNASON (1961) has developed a quasi-barotropic model, which was intended in part, to serve as interim device for the prediction of the movement, but not development, of pressure systems at and below the 500-mb surface until baroclinic models were more successful. Some recent tests indicate that this model is slightly better than the divergent one-parameter model at 500 mb and achieves its aim with moderate success at several other levels.

It therefore appears desirable to examine its stability characteristics.

The vorticity equation for the stratified model may be expressed as

$$(\nabla^2 - q^2)\frac{\partial \Psi'}{\partial t} + \mathbf{V} \cdot \nabla(\nabla^2 \Psi' + f) - q^2 \mathbf{V} \cdot \nabla \Psi' = 0, \qquad (16)$$

where $q^2 = f(\nabla^2\Psi' + f)/g''H$, and will be treated

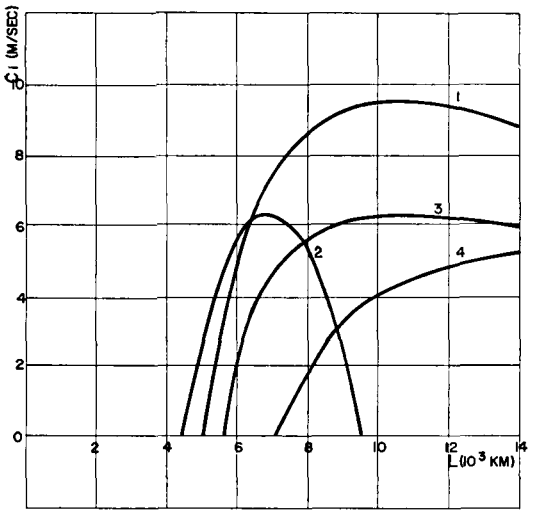

FIG. 14. Similar to figure 3 but for stratified model.

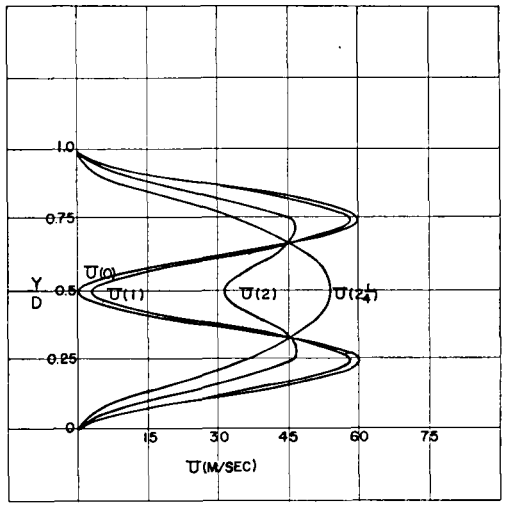

FIG. 15. The zonal wind profile $U = B(1 - \cos(4\pi/D)y)$ initially, U (0), and after 1, 2, and 2 ¼ days with $\beta = \beta_{45}$, $q^2 = 0$, $D = 3000$ km, $L = 3000$ km, $B = 30$ m/sec, A_1 for a perturbation velocity of 5 m/sec and $A_3 = 0$.

as a constant; g'' is a measure of gravity, corrected for compressibility; and $\bar{V}$ is a space-mean wind. Applying the perturbation method leads to the form

$$(\nabla^2 - q^2)\frac{\partial \psi'}{\partial t} + U\frac{\partial}{\partial x}(\nabla^2\psi') + \frac{\partial \psi'}{\partial x} \cdot \left(\beta - \frac{d^2U}{dy_2} - q^2U\right) = 0. \quad (17)$$

Comparison to the analogous divergent one-parameter equations (1) and (2) shows that the above equations have one more term, which may be considered as divergence in addition to the Helmholtz term. According to Arnason this leads to better control of long waves and also can provide for proper movement of systems at levels below 500 mb.

Substituting the harmonic perturbation (3) into (17) gives:

$$(U - c)(\phi'' - \mu^2\phi) + [\beta - U'' + q^2(c - U]\phi = 0, \quad (18)$$

the double prime designating a second derivative with respect to y.

The stability characteristic of this model will be determined by the Fourier method with $N = 5$ for the zonal wind profile

$$U = B\left(1 - \cos\frac{2\pi}{D}y\right).$$

Substitution of (10) and (12) into (18) leads to the same type of frequency equation as (14); however, some of the coefficients differ somewhat as follows:

$$G = \beta - 1/2B(3\mu^2 - \lambda^2 + 3q^2),$$
$$H = 1/2B(5\lambda^2 + \mu^2 + q^2)$$
$$P = 1/2B(\mu^2 + q^2 - 3\lambda^2),$$
$$S = \beta - B(9\lambda^2 + \mu^2 + q^2),$$
$$T = 1/2B(21\lambda^2 + \mu^2 + q^2),$$
$$V = \beta - B(25\lambda^2 + \mu^2 + q^2)$$

Figure 14 gives c_i as a function of L for the stratified model with $D = 4000$ km. These results may be compared to those of the analogous standard one-parameter model, which are given in figure 10. Curves 1 for $\beta = q = 0$, and also curves 2 for $\beta = \beta_{45}$, $q = 0$, are quite similar in the two figures. However, curves 3 and 4 of the stratified model show generally larger values of c_i, a shift of the unstable band toward longer wavelengths and a much broader band of unstable wavelengths. For the wavelengths shown, there were no complex roots in the stratified model corresponding to curve 5 of figure 10; however, such may occur at still larger values of L. Thus, the stratified model displays greater instability than the conventional one-parameter model.

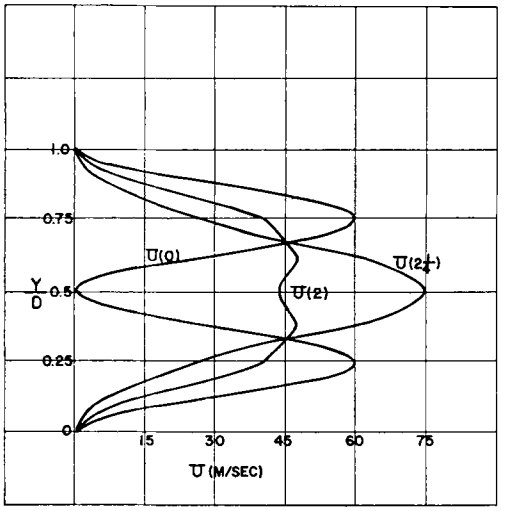

FIG. 16. Similar to figure 15 except that A_3 is same as A_1 there.

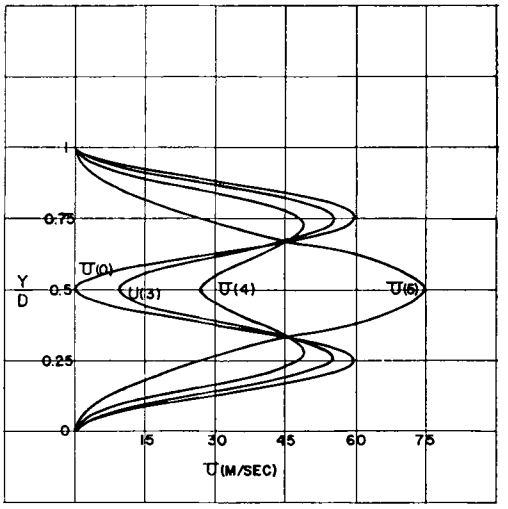

FIG. 17. Similar to figure 16, except that $D = 6000$ km and $L = 4000$ km.

The curves for $D = 2000$ for this model are not given here but are somewhat like those of figure 13 and, in general, revealed greater instability than the broader basic current represented by figure 14.

6. Momentum transfer

In WIIN-NIELSEN's paper (1961) it was shown that a single-jet basic current tends to split into double-jet flow as a result of the meridional convergence of momentum transfer by the unstable eddies. This result was based on the roots of the frequency equation derived for the basic flow. However, as the basic flow is modified by the momentum transfer, the profile may be altered so radically that the solution to the initial perturbation pattern no longer applies. As a matter of fact, Wiin-Nielsen, using a different method suggested by E. N. Lorenz, presented additional computations showing an oscillation from single to double-jet and vice versa. Nevertheless, it may be of some interest to utilize the solutions presented here for the double-jet profile and determine the time required for transition to a single-jet from the results of the linear theory. Combining the equation of motion in the x-direction and the equation of continuity and taking the average over one wavelength leads to the result

$$\frac{\partial u}{\partial t} = -\frac{\partial (u'v')}{\partial y}. \qquad (18)$$

Next the perturbation stream function (3) is used to determine the wind components u' and v' for evaluation of the right hand member of (18). The ϕ_j and corresponding c_j are obtainable from the linear homogeneous system of equations for the ϕ_j and the associated frequency equation. For example, for the single jet with $N = 5$, the required equations are (13) and (14). For comparison to Wiin-Nielsen's results for the single jet with $N = 3$, the computations have been carried out here for the double-jet given by (15) with $B = 30$ m/sec and $N = 3$. The basic derivation is the same as that given by Wiin-Nielsen, only the various coefficients, phase velocities, and amplitudes are different. The initial perturbation is taken as

$$\phi = A_1 \sin(\pi y/D) + A_3 \sin(3\pi y/D). \qquad (18)$$

The results for the double-jet basic current are shown in figures 15, 16 and 17. Figure 15 gives U as a function of time for the non-divergent model ($q = 0$) with $\beta = \beta_{45}$, $D = 3000$ km, $L = 2000$ km, an A_1 which gives a perturbation velocity of 5 m/sec, and $A_3 = 0$. The wavelength of 2000 km corresponded to maximum instability when $D = 3000$ km, with $c = (28.9 \pm 3.9i)$ m/sec. During the first day there was little change; however, by the end of the second day the zonal wind at the center of the channel had increased markedly, and by $2\frac{1}{2}$ days the transition from a double-jet to a single-jet current had been completed.

Figure 16 is similar to 15 except that $A_3 = 5$ m/sec also. Here the transition is even more rapid with the jet becoming stronger and more sharply peaked by $2\frac{1}{4}$ days.

Finally, figure 17 depicts the non-divergent case for a broader current with $D = 6000$ km, $L = 4000$ km and the other parameters the same as in figure 16. As might be expected the period for transition from double to single-jet is much longer.

It follows from the last three diagrams that if there exists barotropic instability in a basic current exhibiting a double-jet structure, meridional convergence of momentum by the unstable eddies will tend to transform the velocity profile into a single-jet zonal wind.

7. Summary and conclusions

The dynamic stability of single-jet and double-jet zonal currents is investigated for several quasi-barotropic models by two approximations, namely, a finite difference technique and a finite Fourier series method. In general the two methods give similar results but some moderate differences occur when the finite difference mesh length or the number of Fourier components is varied. Also the stability characteristics of the various single- and double-jet profiles studied differed considerably.

The Helmholtz divergence term by and large tends to reduce the instability in the single-jet currents; however, the reverse was usually found for the double-jet current, particularly in the longer wavelengths. The instability also tends to decrease with increasing width of the basic current.

Arnason's stratified model is found to be more unstable than the conventional one-parameter barotropic model.

In the last section it is found by linear theory that a double-jet basic current tends to be transformed into a single-jet current in a few days as a result of the meridional convergence of momentum transfer by unstable perturbations.

REFERENCES

ARNASON, G., 1961: A Study of the Dynamics of a Stratified Fluid in Relation to Atmospheric Motions and Physical Prediction, *Tellus*, **13**, pp. 156–170.

ELIASSEN, E. 1954: Numerical Solutions of the Perturbation Equation for Linear Flow, *Tellus*, **6**, pp. 183–192.

KUO, H. L., 1949: Dynamic Instability of Two-Dimensional Non-Divergent Flow in a Barotropic Atmosphere, *Journal of Meteorology*, Vol. **6**, pp. 105–122.

MULLER, D. E., 1956: A Method for Solving Algebraic Equations Using an Automatic Computer, *Mathematical Tables and other Aids to Computation*, Vol. **10**, No. 56, pp. 208–215.

WIIN-NIELSEN, A., 1959: On Barotropic and Baroclinic Models, with Special Emphasis on Ultra-Long Waves, *Monthly Weather Review*, **87**, pp. 171–183.

WIIN-NIELSEN, A., 1961: On Short and Long Term Variations in Quasi-Barotropic Flow, *Monthly Weather Review*, **89**, pp. 461–406.